Results

Effects of PEDF on Serum Starvation-Induced Apoptosis in R28 Cultures

The R28 cell line was derived from the rat retina on postnatal day 6 and has been shown to express neuronal genes.[29] To investigate whether PEDF can act as a survival factor for R28, we first cultured R28 cells under a serum-starved condition with or without rhPEDF, and assessed the cell viability by WST-8 colorimetric assay after 48 hours of culturing. Treatment with rhPEDF dose dependently rescued serum starvation-induced cell death and 41.1% of the reduction of cell viability was rescued by 2500 ng/ml rhPEDF ($P < 0.01$ versus PBS-treated R28 cells; Figure 1A). The effect of rhPEDF was completely reversed by treatment with polyclonal anti-hPEDF antibodies (25 μg/ml) (Figure 1A). The vitreous of the human eye contains 0.5 to 5 μg/ml of hPEDF protein,[30,31] and thus the concentrations of rhPEDF used in this experiment were in a physiological range. TUNEL staining revealed that ~10% of cells were TUNEL-positive apoptotic cells after 48 hours of serum starvation (12.2 ± 1.13%); by contrast, treatment with rhPEDF significantly reduced the frequency of TUNEL-positive cells (5.1 ± 0.26%, $P = 0.0002$; Figure 1, B and C). Less than 2% of cells were TUNEL-positive under control conditions. The apoptotic population was also assessed by fluorescence-activated cell sorter analysis of Annexin V/7-AAD staining. The percentages of early apoptotic cells that were defined as Annexin V-PE-positive and 7-AAD-negative were significantly lower in rhPEDF-treated cells (17.7 ± 0.34%) than PBS-treated cells (28.3 ± 0.15%, $P < 0.0001$; Figure 1D). Together, these results indicate that PEDF inhibits the apoptosis induced by serum starvation in R28 cells. RT-PCR analysis revealed that R28 cells strongly expressed the PEDF receptor, which was identified in a recent study (data not shown).[32]

A Minor Role of Caspases in Serum Starvation-Induced Apoptosis in R28 Cells

To elucidate the molecular events during serum starvation-induced apoptosis, we next examined the involvement of caspases. First, we performed Western blot analysis of caspase-3, a key effector of caspase-dependent apoptosis. As shown in Figure 2A, a 17-kDa active form of caspase-3 was detected at 48 hours after serum starvation. To elucidate the exact contribution of caspases, we next cultured R28 cells under a serum-starved condition, in the presence or absence of Z-VAD-fmk, a broad range caspase inhibitor. Treatment with Z-VAD-fmk (10 μmol/L) completely abrogated the cleavage of caspase-3 induced by serum starvation (Figure 2A), but this treatment showed no beneficial effect on the cell viability (Figure 2B). The doses higher than 10 μmol/L were cytotoxic, reducing the levels of cell viability (data not shown). These results suggest that caspases are not the major executioners of serum starvation-induced apoptosis. By contrast, the cell death induced by staurosporine, a potent activator of caspases, was significantly rescued by treatment with Z-VAD-fmk (10 μmol/L) (Figure 2C). Interestingly, rhPEDF had no significant effect on either the cell viability or the cleavage of caspase-3 after staurosporine treatment (Figure 2, C and D), suggesting that PEDF might be involved in a caspase-independent pathway.

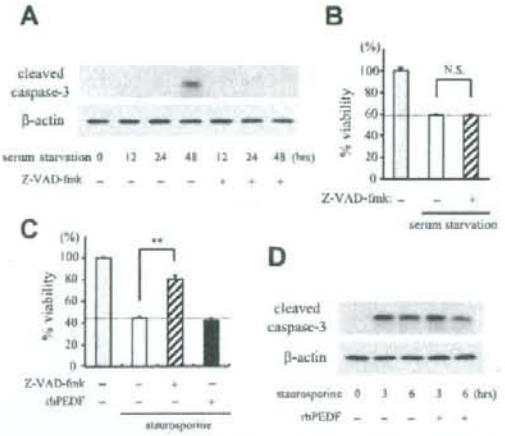

Figure 2. The role of caspases in serum starvation-induced apoptosis. **A:** Analysis of activation of caspase-3 after serum starvation. Total proteins were purified from R28 cells that were serum-deprived for the indicated period of time with or without Z-VAD-fmk (10 μmol/L), and subjected to Western blotting with an antibody against cleaved caspase-3 (**top**). Lane-loading differences were normalized by the level of β-actin (**bottom**). The panels show the representative results from three independent experiments. **B:** The inhibition of caspases did not rescue serum starvation-induced cell death. R28 cells were cultured under a serum-starved condition for 48 hours in the presence or absence of Z-VAD-fmk (10 μmol/L) before assessing the cell viability ($n = 4$ each). **C:** Staurosporine-induced cell death was rescued by Z-VAD-fmk, but not by PEDF. R28 cells were cultured with 100 nmol/L staurosporine for 24 hours in the presence of PBS, Z-VAD-fmk (10 μmol/L), or rhPEDF (2500 ng/ml), and the cell viability was assessed ($n = 4$ each). $^{**}P < 0.01$. **D:** The effect of PEDF on caspase-3 activation induced by staurosporine. Total proteins were purified from R28 cells that were treated with staurosporine for the indicated period of time with or without rhPEDF (2500 ng/ml). Western blotting showed that the expression level of cleaved caspase-3 was unchanged by rhPEDF.

Role of AIF in Serum Starvation-Induced Apoptosis and Effects of PEDF on AIF Relocalization

AIF is a mitochondrial flavoprotein that is released in response to death stimuli and induces apoptosis independently of caspases after nuclear translocation.[20] To examine whether serum starvation-induced apoptosis involved AIF, we next analyzed the changes in subcellular localization of AIF by immunocytochemistry. In control R28 cells, AIF was excluded from the nucleus and displayed a punctate staining pattern in the cytoplasm. By contrast, after 48 hours of serum starvation, 17.5 ± 4.6% of the cells showed diffuse staining and nuclear translocation of AIF (Figure 3, A and B). No positive staining was found by nonimmune IgG (data not shown). Double-labeling with TUNEL showed that ~75% of AIF-positive nuclei were also TUNEL-positive (Figure 3, C and D). Furthermore, treatment with rhPEDF dramatically pre-

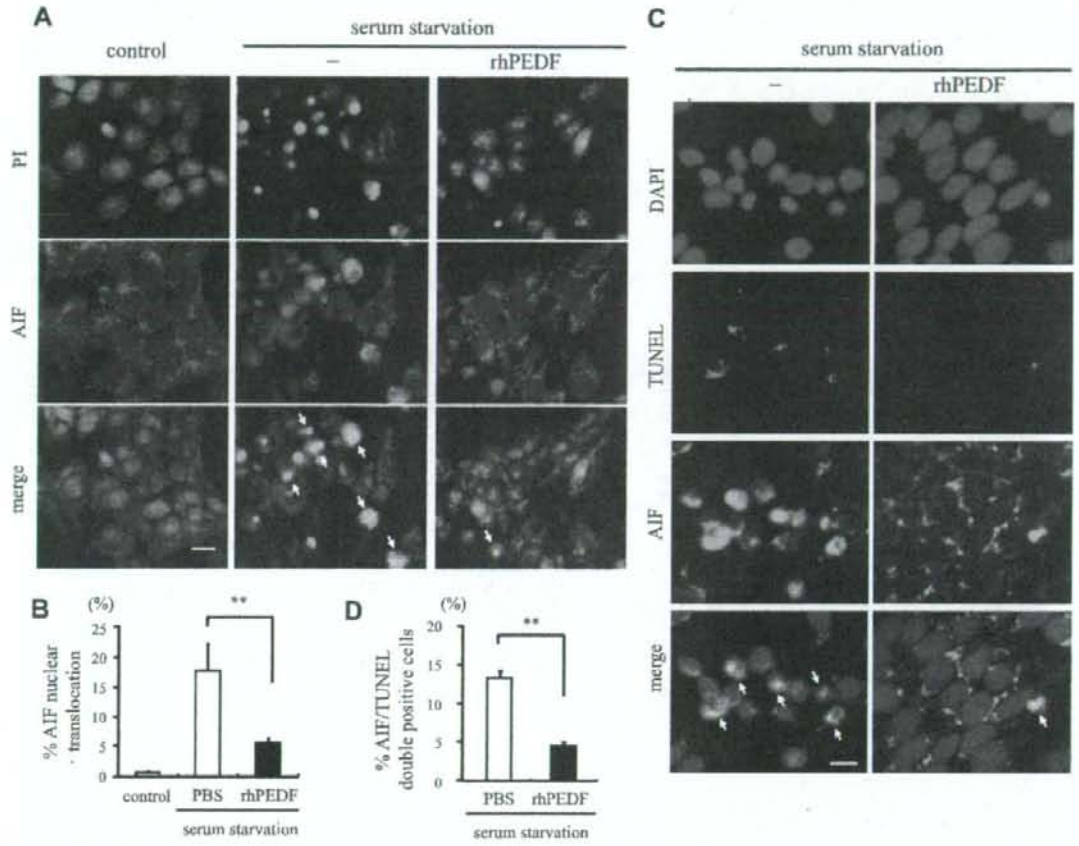

Figure 3. AIF nuclear translocation during serum starvation-induced apoptosis and effect of PEDF on the AIF release. **A:** Immunocytochemistry of AIF after serum starvation. After 48 hours of culturing in serum-starved medium with or without rhPEDF (2500 ng/ml), the R28 cells were stained with an anti-AIF antibody. The cells growing in serum-containing medium were used as controls. The nuclei were counterstained with propidium iodide. **Arrows** indicate the translocation of AIF into the nucleus. **B:** Quantification of cells showing nuclear translocation of AIF in control (gray bar) or serum-starved R28 cells treated with PBS (white bar) or rhPEDF (black bar) ($n = 5$ each). $^{**}P < 0.01$. **C** and **D:** Double-staining for AIF and TUNEL (**C**) and the quantification of AIF/TUNEL double-positive apoptotic nuclei (**D**) after serum starvation ($n = 5$ each). The nuclei were counterstained with DAPI. **Arrows** indicate the co-localization of AIF and TUNEL. $^{**}P < 0.01$. Scale bars = 10 μm.

vented the nuclear translocation of AIF after serum starvation (5.6 ± 0.74%, $P = 0.0066$ versus PBS-treated samples; Figure 3, A and B) and reduced the number of AIF/TUNEL double-positive cells ($P < 0.0001$ versus PBS-treated samples; Figure 3, C and D).

To further address the role of AIF in serum starvation-induced apoptosis, we used RNAi to knockdown AIF in R28 cells. siRNA for AIF, but not randomized control siRNA, showed efficient down-regulation of AIF (Figure 4A). When AIF was down-regulated, 33.1% of the reduction of cell viability after 48 hours of serum starvation was rescued ($P = 0.0002$ versus R28 cells treated with randomized control siRNA; Figure 4B). TUNEL-positive apoptotic cells were also significantly reduced in cells treated with siRNA for AIF (6.6 ± 1.30%) compared to cells treated with randomized control siRNA (13.6 ± 0.76%, $P = 0.0031$; Figure 4, C and D). In addition, treatment with rhPEDF showed no significant effect on the frequency of TUNEL-positive cells in samples with AIF down-regulation (5.39 ± 1.11%, $P = 0.53$; Figure 4, C and D). Together, these results indicate that AIF is an important executioner of serum starvation-induced apoptosis, and that PEDF inhibits the apoptosis by preventing the AIF nuclear translocation.

PEDF Prevents AIF Translocation and Photoreceptor Apoptosis in RCS Rats

To further examine the role of PEDF *in vivo*, we next assessed the effect of exogenously overexpressed PEDF on the degeneration of photoreceptors in RCS rats. P21 RCS rats received subretinal injection of SIV-hPEDF or SIV-Empty in the nasal peripheral retinas. First, we confirmed the efficient gene transfer and expression of hPEDF after subretinal injection of SIV-hPEDF by ELISA (Figure 5A). The gene transfer of hPEDF was observed in the RPE in the vector-injected area as previously de-

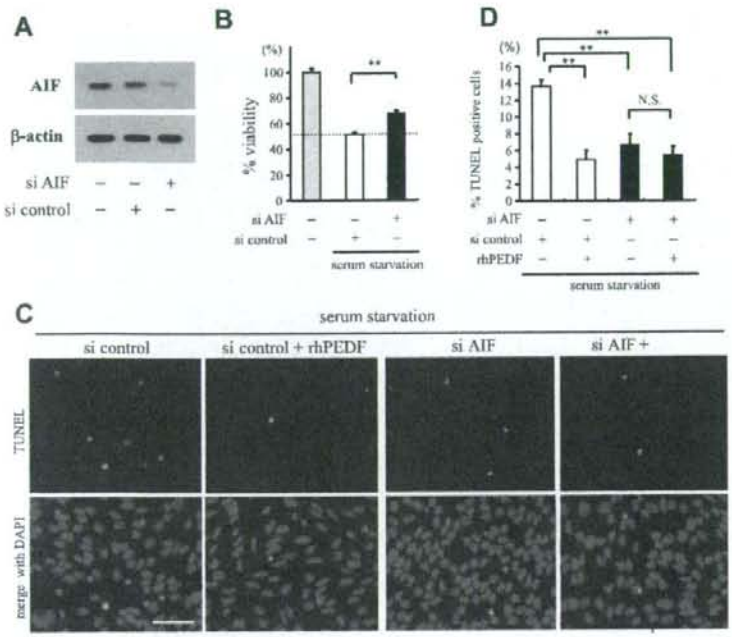

Figure 4. Knockdown of AIF mRNA rescues R28 apoptosis after serum starvation. **A:** Western blot analysis for AIF in RNAi experiments. Total proteins were purified from R28 cells 48 hours after transfection of siRNA for AIF or randomized control siRNA (**top**). Lane-loading differences were normalized by the level of β-actin (**bottom**). The panels show the representative results from three independent experiments. **B:** The siRNA targeting AIF or randomized control siRNA were transfected to R28 cells before the serum starvation assay. The cell viability was assessed after culturing in serum-free medium for 48 hours ($n = 4$ each) $^{**}P < 0.01$. **C** and **D:** TUNEL staining (**C**) and quantitative analysis of the TUNEL-positive cells (**D**) in serum-starved R28 cells treated with randomized control siRNA (white bar) or siRNA targeting AIF (black bar) and the effect of rhPEDF (2500 ng/ml) on these cells ($n = 5$ each). $^{**}P < 0.01$. Scale bar = 50 μm.

scribed (data not shown).[11] At 2 weeks after the gene transfer, the number of photoreceptors was counted per 100 μm at 10 points along the horizontal meridian of the eyes. As shown in Figure 5, B and C, the retinas treated with SIV-hPEDF demonstrated significant rescue of photoreceptors in the nasal hemisphere, compared to retinas that were untreated or treated with SIV-Empty ($P < 0.05$). The region nearest the vector-injected site (A1 to A3) showed the greatest prevention of photoreceptor cell death, and thus we assessed the retinas in areas A1 to A3 in the following experiments. The percentage of TUNEL-positive photoreceptor nuclei in the outer nuclear layer was ~3.5% in the untreated or SIV-Empty-treated retinas, whereas it was significantly decreased in the SIV-hPEDF-treated retinas (0.8 ± 0.07%, $P < 0.01$; Figure 5, D and E). Throughout the study period, neither severe inflammation nor morphological change of RPE was seen in any of the retinas. Next, we conducted double-staining of AIF and TUNEL in these retinas. Immunohistochemistry of control normal retinas showed a positive staining for AIF in the inner segment (IS) of photoreceptors, which were a mitochondrion-rich portion of cells. In RCS rats that were untreated or treated with SIV-Empty, the AIF distribution in the IS was disrupted and AIF translocation was observed in most of the TUNEL-positive nuclei (percentage of AIF/TUNEL double-positive nuclei: 3.4 ± 0.38% and 3.2 ± 0.56%, respectively). By contrast, treatment with SIV-hPEDF relatively preserved the distribution and significantly reduced the AIF translocation into the nuclei (0.6 ± 0.05%, $P < 0.01$; Figure 6). At 4 weeks after the gene transfer, the SIV-hPEDF-treated retinas also showed the reduction of AIF nuclear translocation and had more than twice the number of photoreceptor nuclei compared to untreated or SIV-Empty-treated retinas. However, the number of photoreceptors was reduced by half in comparison with that at 2 weeks after vector injection, indicating that the retinal degeneration was delayed but not completely prevented by the gene transfer of hPEDF (see Supplementary Figure S1 at *http://ajp.amjpathol.org*). These findings were consistent with the *in vitro* data, and indicate that PEDF prevents the translocation of AIF, resulting in a substantial protection of photoreceptors during retinal degeneration.

PEDF Prevents AIF Translocation through Bcl-2 Up-Regulation

During apoptosis, AIF is released after the loss of mitochondrial membrane potential,[33] and this release is inhibited by overexpression of Bcl-2, which preserves the mitochondrial integrity.[15,34] Based on the findings that PEDF prevents AIF translocation both *in vitro* and *in vivo*, we finally asked whether PEDF affects the mitochondrial function and the expression of pro- and anti-apoptotic Bcl-2 family members. To examine the changes in mitochondrial membrane potential during serum starvation-induced apoptosis, R28 cells were co-cultured with a mitochondrial potential-sensitive dye, MitoTracker CMTMRos. In control R28 cells, the mitochondria exhibited a punctate staining pattern with MitoTracker CMTMRos. After 48 hours of serum starvation, 16.7 ± 2.60% of the cells showed the loss of MitoTracker staining, indicating the mitochondrial depolarization. This effect was significantly reversed by rhPEDF treatment (4.9 ± 1.29%, $P = 0.0068$; Figure 7A). Next, we assessed the transcriptional

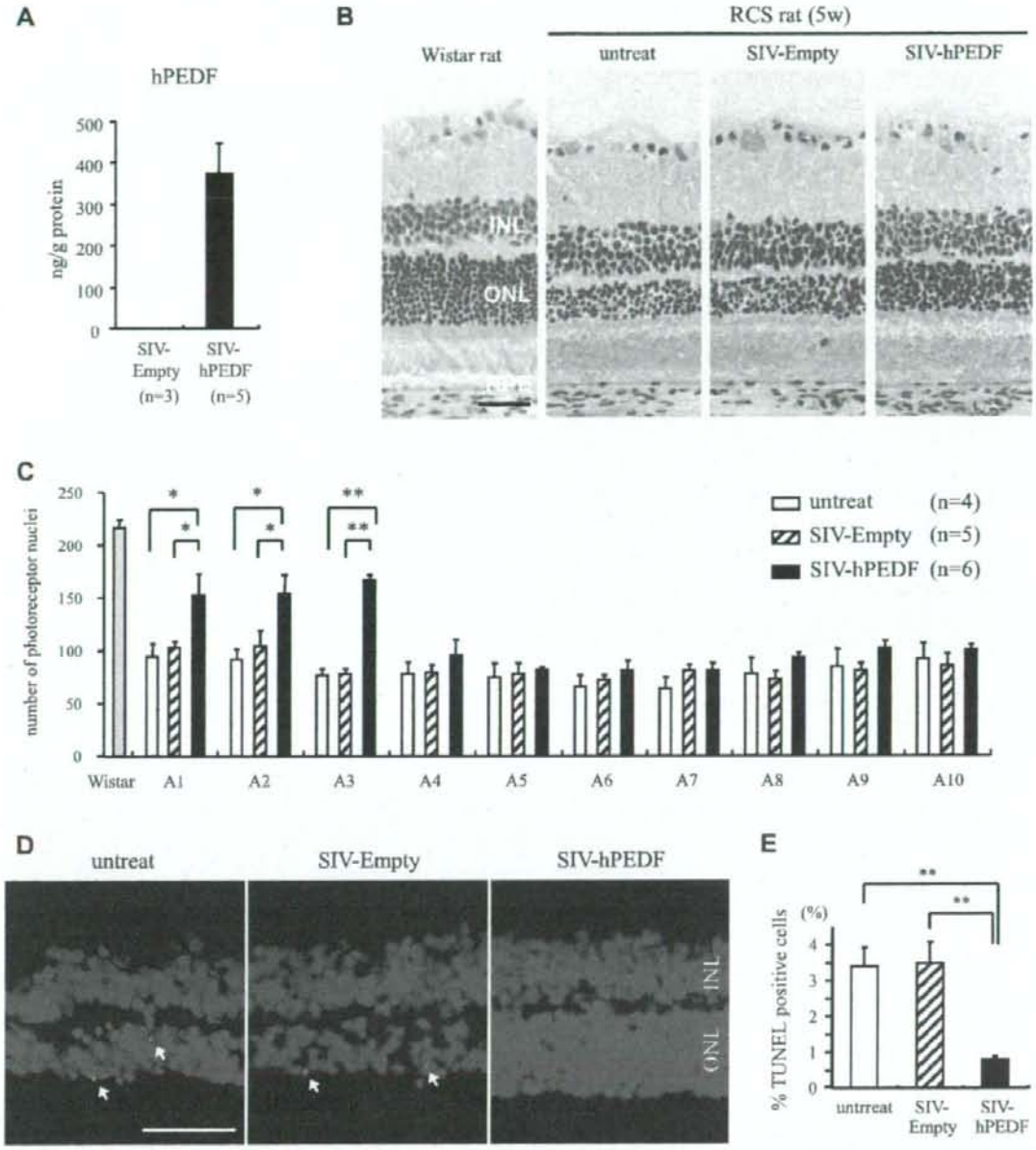

Figure 5. SIV vector-mediated retinal gene transfer of PEDF prevents photoreceptor apoptosis in RCS rats. **A:** ELISA to detect hPEDF protein at 2 weeks after subretinal injection of SIV-hPEDF into the nasal peripheral retinas of RCS rats ($n = 3$ to 5). **B:** Histological findings of the nasal retina of untreated RCS rats, and RCS rats treated with SIV-Empty or SIV-hPEDF at 2 weeks after injection. The retinas of Wistar rats were used as a control. INL, inner nuclear layer; ONL, outer nuclear layer. RPE indicates retinal pigment epithelium, which lie at the outer layer of retina. **C:** Quantitative analysis of photoreceptor nuclei in RCS rats. The number of photoreceptors per 100 μm was counted at 10 points along the horizontal meridian of the eye (A1 to A10) ($n = 4$ to 6). The region A1 to A5 corresponds to the nasal hemisphere of the eye. $^*P < 0.05$ and $^{**}P < 0.01$. **D** and **E:** TUNEL staining (**D**) and quantitative analysis of the TUNEL-positive photoreceptor nuclei (**E**) in RCS rats at 2 weeks after vector injection ($n = 4$ to 6). $^*P < 0.05$ and $^{**}P < 0.01$. Scale bars = 50 μm. The **arrows** indicate the TUNEL-positive photoreceptor nuclei.

changes in Bax and Bcl-2 expression by quantitative real-time PCR. In R28 cells, treatment with rhPEDF resulted in a 1.7-fold increase of Bcl-2 expression at 6 hours after stimulation ($P = 0.0206$ versus PBS-treated samples; Figure 7B). The level of Bax expression was almost unchanged. In RCS rats, Bcl-2 expression increased twofold in the neural retina treated with SIV-hPEDF, compared to that in untreated or SIV-Empty-treated rats ($P < 0.03$; Figure 7C). Western blot analysis confirmed that the protein expression of Bcl-2 was up-

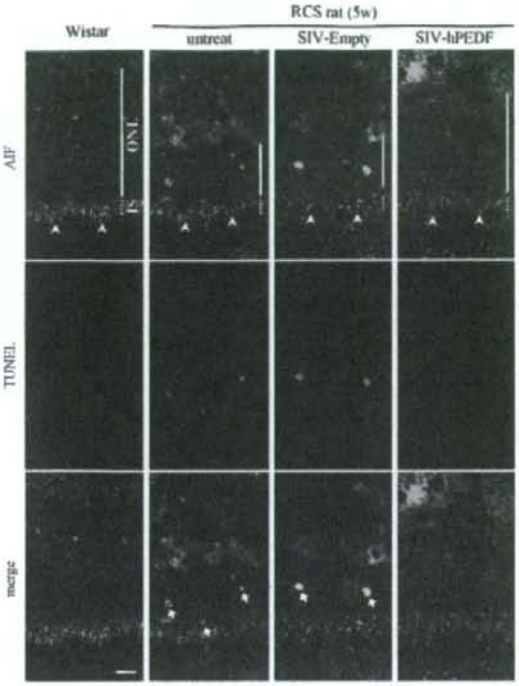

Figure 6. PEDF inhibits AIF translocation in photoreceptors of RCS rats. Confocal microscopy of the nasal retina double-stained with AIF and TUNEL at 2 weeks after vector injection. The **arrowheads** indicate the distribution of AIF in the IS of photoreceptors and the **arrows** indicate the co-localization of AIF and TUNEL. Scale bar = 10 μm.

regulated in R28 cells and the eyes of RCS rats by treatment with PEDF (Figure 7, D and E). To further examine the role of Bcl-2 in the PEDF-mediated inhibition of AIF release, we performed knockdown experiments in R28 cells. siRNA for Bcl-2, but not control siRNA, showed efficient down-regulation of Bcl-2 (Figure 7F), and attenuated the effect of PEDF on AIF nuclear translocation after serum starvation (Figure 7, G and H). Together, these data indicate that PEDF prevents the loss of mitochondrial membrane potential and inhibits AIF nuclear translocation by inducing Bcl-2 expression.

Discussion

Molecular genetic analyses of inherited retinal degeneration have identified 40 different genetic mutations accounting for only a minority of RP patients [Retinal Information Network (RetNet) at *http://www.sph.uth.tmc.edu/Retnet/*]. Despite advances in our understanding of the genetic heterogeneity of RP, the mechanism by which photoreceptors execute apoptosis is primarily unknown and is a matter of continuing debate. In the present study, we investigated the signaling pathways that are directly related to the neuroprotective activity of PEDF in retinal degeneration. The key observations made in this study are as follows: i) PEDF efficiently rescued apoptosis induced by serum starvation but not by staurosporine in R28 cells derived from rat retina; ii) AIF but not caspases was a key effector of the serum starvation-induced apoptosis, and PEDF prevented AIF from translocating into the nucleus after serum starvation; iii) Nuclear translocation of AIF was also observed in apoptotic photoreceptors of RCS rats, and was significantly inhibited by retinal gene transfer of PEDF *in vivo*, resulting in a substantial delay in retinal degeneration; and iv) PEDF prevented the AIF release through up-regulation of Bcl-2. These findings clearly demonstrated that the AIF-mediated pathway is an essential target of PEDF during the photoreceptor apoptosis in retinal degeneration.

There has been an increasing body of evidence suggesting that caspases are not essential for photoreceptor apoptosis in animal models of retinal degeneration. In the mature brain and retina, it has been demonstrated that caspase-dependent apoptosis is down-regulated because of a differentiation-associated reduction in apoptosis proteases-activating factor-1 expression and increased efficacy of inhibitors of apoptosis proteins.[35–37] Segura and colleagues[38] recently reported that the long form of the Fas apoptotic inhibitory molecule is predominantly expressed in neurons and prevents the activation of caspase-8 induced by Fas. During photoreceptor apoptosis in rd1 mice or light-induced retinal injury, caspases were not activated and the apoptosis was not prevented by a broad-range caspase inhibitor or gene ablation of caspase-3.[36,39–41] We also observed that treatment with Z-VAD-fmk showed no significant protective effect on retinal degeneration in RCS rats (see Supplementary Figure S2 at *http://ajp.amjpathol.org*). These findings strongly suggest the presence of a caspase-independent mechanism in retinal degeneration; however, it has remained unclear which pathways are actually involved in the apoptotic process. In the present study, we demonstrated for the first time that nuclear translocation of AIF was observed in apoptotic photoreceptors of RCS rats, which carry a mutation of the receptor tyrosine kinase *Mertk* (Figure 6). Recently, Sanges and colleagues[41] reported that AIF also significantly contributes to photoreceptor apoptosis in rd1 mice, which is caused by a mutation in the gene for the β-subunit of rod photoreceptor cGMP phosphodiesterase *PDE6B*, and thus it may be possible that nuclear translocation of AIF is a common pathway in inherited retinal degeneration irrespective of the genetic status. Further studies will be needed to clarify the role of AIF in other models of retinal degeneration with different mutations.

In culture, we showed that R28 cell apoptosis induced by serum starvation could occur independently of caspase activation. The cell death was not rescued by the broad range caspase inhibitor Z-VAD-fmk (Figure 2B). It is unlikely that the caspase blockade was insufficient under this condition, because the activation of caspase-3 after serum starvation was completely abrogated and the cell death induced by staurosporine was significantly rescued by treatment with Z-VAD-fmk (Figure 2, A and C). By contrast, many of the apoptotic cells showed nuclear translocation of AIF, and siRNA-mediated knockdown of AIF resulted in a significant rescue of the apoptosis (Figures 3 and 4). Consistent with our

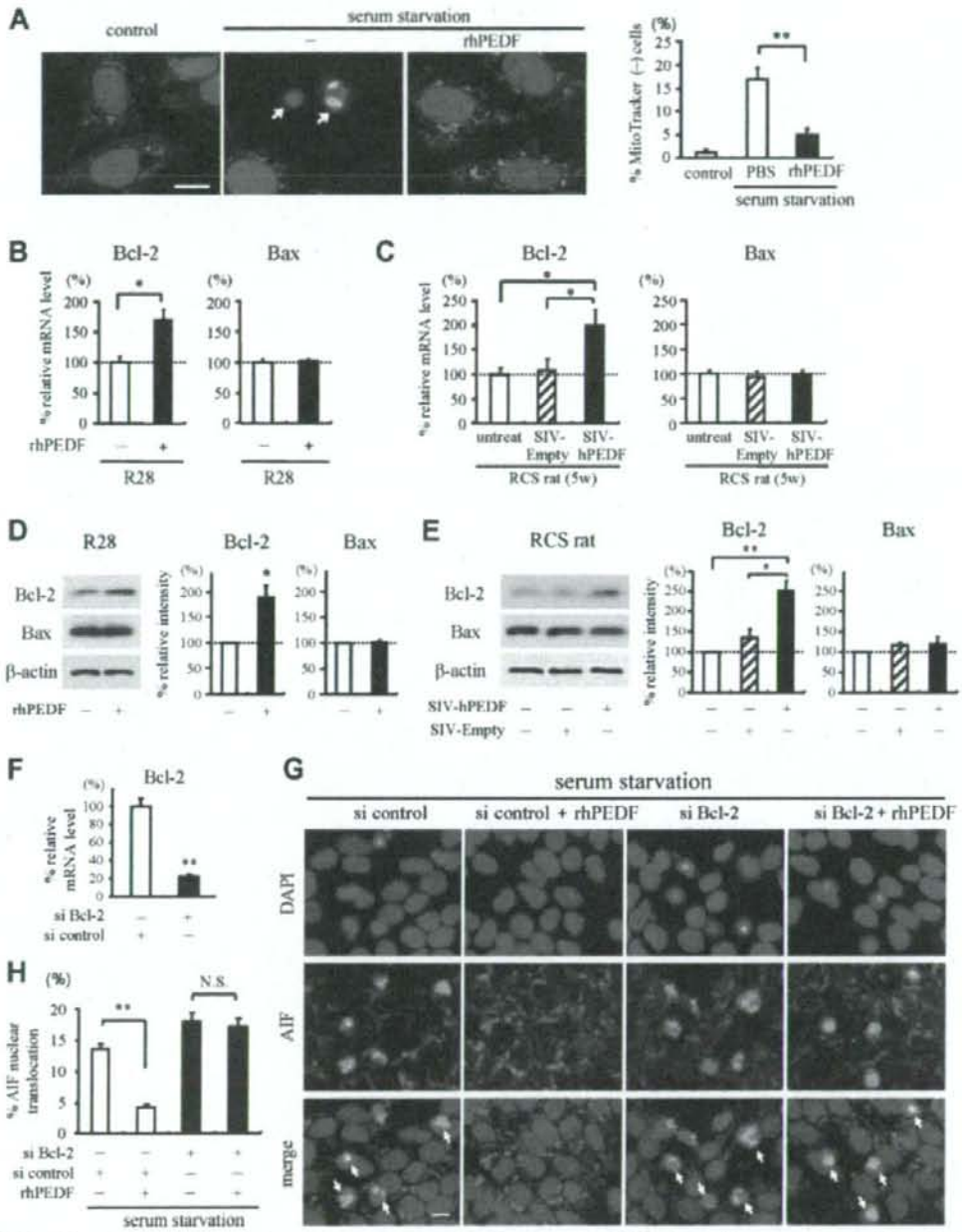

Figure 7. The effect of PEDF on mitochondrial function and expression of Bcl-2 family members. **A:** Mitochondrial function was assessed by a mitochondrial membrane potential-sensitive dye, MitoTracker CMTMRos. MitoTracker intake (MitoTracker in red, DAPI in blue) was lost in pyknotic R28 cells after 48 hours of serum starvation (**arrows**), but reversed in cells treated with rhPEDF (2500 ng/ml). The **right** panel shows the quantified results. $^{**}P < 0.01$. **B** and **C:** Quantitative real-time PCR analysis for Bcl-2 and Bax in PEDF-treated R28 cells (**B**) and neural retinas of RCS rats (**C**). **B:** R28 cells treated with rhPEDF or PBS were harvested and subjected to quantitative real-time PCR analysis at 6 hours after stimulation ($n = 4$ each). $^{*}P < 0.05$. **C:** At 2 weeks after vector injection, the neural retinas of untreated RCS rats or RCS rats treated with SIV-Empty or SIV-hPEDF were subjected to quantitative real-time PCR analysis ($n = 5$ to 6). $^{**}P < 0.05$. **D** and **E:** Western blot analysis for Bcl-2 and Bax in R28 cells after 24 hours of rhPEDF treatment (**D**) and in the eyes of RCS rats at 2 weeks after vector injection (**E**). Lane-loading differences were normalized by the level of β-actin. The bar graphs indicate the relative level of Bcl-2 or Bax to β-actin by densitometric analysis, reflecting the results from three independent experiments. $^{*}P < 0.05$ and $^{**}P < 0.01$. **F:** Quantitative real-time PCR analysis for Bcl-2 in R28 cells transfected with control siRNA or siRNA targeting Bcl-2 ($n = 3$ each). $^{**}P < 0.01$. **G** and **H:** Immunocytochemistry of AIF (**G**) and quantitative analysis of cells showing AIF nuclear translocation (**H**). Down-regulation of Bcl-2 in R28 cells attenuated the effect of PEDF on AIF nuclear translocation after serum starvation. Scale bars = 10 μm. The **arrows** indicate the cells showing AIF nuclear translocation.

findings, Klein and colleagues[17] reported that the primary granule cells derived from *Harlequin* (*Hq*) mutant mice, in which the AIF expression is reduced to 20% by proviral insertion, are resistant to cell death induced by serum starvation but not to cell death induced by staurosporine. These data suggest that AIF plays an essential role in serum starvation-induced apoptosis. Nuclear translocation of AIF is induced by several death stimuli after mitochondrial outer membrane permeability.[33,42,43] Although the mechanism leading to AIF release is still elusive, recent studies have demonstrated that AIF must be cleaved to be released from mitochondria, unlike other toxic proteins in the mitochondrial intermembrane space.[43,44] It has been shown that proteases such as calpains or cathepsins are involved in AIF cleavage and subsequent neuronal cell death,[45–47] and these proteases might play a role in triggering AIF release after serum starvation.

More interestingly, our data showed that PEDF dramatically prevents the translocation of AIF, resulting in significant inhibition of apoptosis in RCS rats and serum-starved R28 cells. The intracellular signaling pathways by which PEDF acts on neuronal cells have been explored mainly in culture, and the participation of NF-κB and cAMP-responsive element binding protein pathways has been demonstrated[13,48]; however, very little information is available regarding the downstream target molecules. An important advance of the current study, therefore, was that AIF was identified as an essential target molecule during PEDF-mediated neuroprotection both *in vitro* and *in vivo*. Moreover, we showed that the effect of PEDF on the AIF nuclear translocation is mediated by up-regulation of Bcl-2 expression (Figure 7), which directly regulates the mitochondrial membrane permeability and the AIF release.[15,49] However, it is less clear how PEDF up-regulates Bcl-2 gene expression. Notari and colleagues[32] recently determined that adipose triglyceride lipase (ATGL) is a receptor of PEDF and this interaction stimulates the enzymatic phospholipase A_2 (PLA_2) activity of ATGL. Although ATGL plays an essential role for triglyceride catabolism in adipose tissue, liver, and muscles,[50–52] its role in neuronal tissues remains elusive. Because PLA_2 generates free fatty acid and lysophospholipids from membrane phospholipids and modulates neural cell functions including signal transduction and gene transcription,[53] the upstream mechanisms by which PEDF initiates the signaling cascade should be addressed in future studies.

The nuclear translocation of AIF has been shown to be involved in several types of neurodegeneration,[42,54,55] whereas AIF, which is embedded in the inner mitochondrial membrane, exerts a vital function in bioenergetic and redox metabolism in the healthy state.[17,18,56] The persistent down-regulation of its expression might not be feasible for neurons, because *Hq* mutant mice develop specific degeneration of neurons in the cerebellum and retina[17] and forebrain-specific AIF-null mice are embryonic lethal.[20] Therefore, the therapeutic approach using PEDF, which inhibits the AIF release, may be a reasonable strategy for retinal degeneration and other central nervous system diseases. Because the majority of RP diseases in human patients progress over several decades, the delay of the disease progression by PEDF may provide sufficient therapeutic benefits for patients with RP.

In conclusion, we have demonstrated that inhibition of the nuclear translocation of AIF is essential for the neuroprotective activity of PEDF in retinal degeneration. PEDF inhibits the AIF nuclear translocation via up-regulation of Bcl-2, leading to prevention of the photoreceptor apoptosis in RCS rats. These findings indicate that AIF is an essential effector molecule of photoreceptor apoptosis in inherited retinal degeneration, and that the blockade of the AIF release by PEDF may be a useful therapeutic strategy for retinal degenerative diseases such as RP.

Acknowledgments

We thank Drs. Eiji Akiba, Katsuyuki Mitomo, Toshiaki Tabata, and Makoto Inoue for their excellent technical assistance in vector construction and large-scale production; and Mr. Hiroshi Fujii, Miss Chie Arimatsu, and Fumie Doi for their assistance with the experiments.

References

1. Rebello G, Ramesar R, Vorster A, Roberts L, Ehrenreich L, Oppon E, Gama D, Bardien S, Greenberg J, Bonapace G, Waheed A, Shah GN, Sly WS: Apoptosis-inducing signal sequence mutation in carbonic anhydrase IV identified in patients with the RP17 form of retinitis pigmentosa. Proc Natl Acad Sci USA 2004, 101:6617–6622
2. Wang DY, Chan WM, Tam PO, Baum L, Lam DS, Chong KK, Fan BJ, Pang CP: Gene mutations in retinitis pigmentosa and their clinical implications. Clin Chim Acta 2005, 351:5–16
3. Portera-Cailliau C, Sung CH, Nathans J, Adler R: Apoptotic photoreceptor cell death in mouse models of retinitis pigmentosa. Proc Natl Acad Sci USA 1994, 91:974–978
4. Wong P: Apoptosis, retinitis pigmentosa, and degeneration. Biochem Cell Biol 1994, 72:489–498
5. Tombran-Tink J, Johnson LV: Neuronal differentiation of retinoblastoma cells induced by medium conditioned by human RPE cells. Invest Ophthalmol Vis Sci 1989, 30:1700–1707
6. Steele FR, Chader GJ, Johnson LV, Tombran-Tink J: Pigment epithelium-derived factor: neurotrophic activity and identification as a member of the serine protease inhibitor gene family. Proc Natl Acad Sci USA 1993, 90:1526–1530
7. Taniwaki T, Becerra SP, Chader GJ, Schwartz JP: Pigment epithelium-derived factor is a survival factor for cerebellar granule cells in culture. J Neurochem 1995, 64:2509–2517
8. Dawson DW, Volpert OV, Gillis P, Crawford SE, Xu H, Benedict W, Bouck NP: Pigment epithelium-derived factor: a potent inhibitor of angiogenesis. Science 1999, 285:245–248
9. Ogata N, Matsuoka M, Imaizumi M, Arichi M, Matsumura M: Decreased levels of pigment epithelium-derived factor in eyes with neuroretinal dystrophic diseases. Am J Ophthalmol 2004, 137:1129–1130
10. Ikeda Y, Goto Y, Yonemitsu Y, Miyazaki M, Sakamoto T, Ishibashi T, Tabata T, Ueda Y, Hasegawa M, Tobimatsu S, Sueishi K: Simian immunodeficiency virus-based lentivirus vector for retinal gene transfer: a preclinical safety study in adult rats. Gene Ther 2003, 10:1161–1169
11. Miyazaki M, Ikeda Y, Yonemitsu Y, Goto Y, Sakamoto T, Tabata T, Ueda Y, Hasegawa M, Tobimatsu S, Ishibashi T, Sueishi K: Simian lentiviral vector-mediated retinal gene transfer of pigment epithelium-derived factor protects retinal degeneration and electrical defect in Royal College of Surgeons rats. Gene Ther 2003, 10:1503–1511
12. Cayouette M, Smith SB, Becerra SP, Gravel C: Pigment epithelium-

derived factor delays the death of photoreceptors in mouse models of inherited retinal degenerations. Neurobiol Dis 1999, 6:523–532
13. Yabe T, Wilson D, Schwartz JP: NFkappaB activation is required for the neuroprotective effects of pigment epithelium-derived factor (PEDF) on cerebellar granule neurons. J Biol Chem 2001, 276:43313–43319
14. Stefanis L: Caspase-dependent and -independent neuronal death: two distinct pathways to neuronal injury. Neuroscientist 2005, 11:50–62
15. Susin SA, Lorenzo HK, Zamzami N, Marzo I, Snow BE, Brothers GM, Mangion J, Jacotot E, Costantini P, Loeffler M, Larochette N, Goodlett DR, Aebersold R, Siderovski DP, Penninger JM, Kroemer G: Molecular characterization of mitochondrial apoptosis-inducing factor. Nature 1999, 397:441–446
16. Susin SA, Daugas E, Ravagnan L, Samejima K, Zamzami N, Loeffler M, Costantini P, Ferri KF, Irinopoulou T, Prevost MC, Brothers G, Mak TW, Penninger J, Earnshaw WC, Kroemer G: Two distinct pathways leading to nuclear apoptosis. J Exp Med 2000, 192:571–580
17. Klein JA, Longo-Guess CM, Rossmann MP, Seburn KL, Hurd RE, Frankel WN, Bronson RT, Ackerman SL: The harlequin mouse mutation downregulates apoptosis-inducing factor. Nature 2002, 419:367–374
18. Vahsen N, Cande C, Briere JJ, Benit P, Joza N, Larochette N, Mastroberardino PG, Pequignot MO, Casares N, Lazar V, Feraud O, Debili N, Wissing S, Engelhardt S, Madeo F, Piacentini M, Penninger JM, Schagger H, Rustin P, Kroemer G: AIF deficiency compromises oxidative phosphorylation. EMBO J 2004, 23:4679–4689
19. Ye H, Cande C, Stephanou NC, Jiang S, Gurbuxani S, Larochette N, Daugas E, Garrido C, Kroemer G, Wu H: DNA binding is required for the apoptogenic action of apoptosis inducing factor. Nat Struct Biol 2002, 9:680–684
20. Cheung EC, Joza N, Steenaart NA, McClellan KA, Neuspiel M, McNamara S, MacLaurin JG, Rippstein P, Park DS, Shore GC, McBride HM, Penninger JM, Slack RS: Dissociating the dual roles of apoptosis-inducing factor in maintaining mitochondrial structure and apoptosis. EMBO J 2006, 25:4061–4073
21. Hisatomi T, Sakamoto T, Murata T, Yamanaka I, Oshima Y, Hata Y, Ishibashi T, Inomata H, Susin SA, Kroemer G: Relocalization of apoptosis-inducing factor in photoreceptor apoptosis induced by retinal detachment in vivo. Am J Pathol 2001, 158:1271–1278
22. Hisatomi T, Nakazawa T, Noda K, Almulki L, Miyahara S, Nakao S, Ito Y, She H, Kohno R, Michaud N, Ishibashi T, Hafezi-Moghadam A, Badley AD, Kroemer G, Miller JW: HIV protease inhibitors provide neuroprotection through inhibition of mitochondrial apoptosis in mice. J Clin Invest 2006, 116:2025–2038
23. Zhu C, Wang X, Huang Z, Qiu L, Xu F, Vahsen N, Nilsson M, Eriksson PS, Hagberg H, Culmsee C, Plesnila N, Kroemer G, Blomgren K: Apoptosis-inducing factor is a major contributor to neuronal loss induced by neonatal cerebral hypoxia-ischemia. Cell Death Differ 2007, 14:775–784
24. Stellmach V, Crawford SE, Zhou W, Bouck N: Prevention of ischemia-induced retinopathy by the natural ocular antiangiogenic agent pigment epithelium-derived factor. Proc Natl Acad Sci USA 2001, 98:2593–2597
25. Murakami Y, Ikeda Y, Yonemitsu Y, Tanaka S, Kondo H, Okano S, Kohno R, Miyazaki M, Inoue M, Hasegawa M, Ishibashi T, Sueishi K: Newly-developed Sendai virus vector for retinal gene transfer: reduction of innate immune response via deletion of all envelope-related genes. J Gene Med 2008, 10:165–176
26. Tsutsumi N, Yonemitsu Y, Shikada Y, Onimaru M, Tanii M, Okano S, Kaneko K, Hasegawa M, Hashizume M, Maehara Y, Sueishi K: Essential role of PDGFRalpha-p70S6K signaling in mesenchymal cells during therapeutic and tumor angiogenesis in vivo: role of PDGFRalpha during angiogenesis. Circ Res 2004, 94:1186–1194
27. Poot M, Zhang YZ, Kramer JA, Wells KS, Jones LJ, Hanzel DK, Lugade AG, Singer VL, Haugland RP: Analysis of mitochondrial morphology and function with novel fixable fluorescent stains. J Histochem Cytochem 1996, 44:1363–1372
28. Deshmukh M, Kuida K, Johnson EM Jr: Caspase inhibition extends the commitment to neuronal death beyond cytochrome c release to the point of mitochondrial depolarization. J Cell Biol 2000, 150:131–143
29. Seigel GM, Sun W, Wang J, Hershberger DH, Campbell LM, Salvi RJ: Neuronal gene expression and function in the growth-stimulated R28 retinal precursor cell line. Curr Eye Res 2004, 28:257–269
30. Ogata N, Nishikawa M, Nishimura T, Mitsuma Y, Matsumura M: Unbalanced vitreous levels of pigment epithelium-derived factor and vascular endothelial growth factor in diabetic retinopathy. Am J Ophthalmol 2002, 134:348–353
31. Duh EJ, Yang HS, Haller JA, De Juan E, Humayun MS, Gehlbach P, Melia M, Pieramici D, Harlan JB, Campochiaro PA, Zack DJ: Vitreous levels of pigment epithelium-derived factor and vascular endothelial growth factor: implications for ocular angiogenesis. Am J Ophthalmol 2004, 137:668–674
32. Notari L, Baladron V, Aroca-Aguilar JD, Balko N, Heredia R, Meyer C, Notario PM, Saravanamuthu S, Nueda ML, Sanchez-Sanchez F, Escribano J, Laborda J, Becerra SP: Identification of a lipase-linked cell membrane receptor for pigment epithelium-derived factor. J Biol Chem 2006, 281:38022–38037
33. Yu SW, Wang H, Poitras MF, Coombs C, Bowers WJ, Federoff HJ, Poirier GG, Dawson TM, Dawson VL: Mediation of poly(ADP-ribose) polymerase-1-dependent cell death by apoptosis-inducing factor. Science 2002, 297:259–263
34. Green DR, Kroemer G: The pathophysiology of mitochondrial cell death. Science 2004, 305:626–629
35. Yakovlev AG, Ota K, Wang G, Movsesyan V, Bao WL, Yoshihara K, Faden AI: Differential expression of apoptotic protease-activating factor-1 and caspase-3 genes and susceptibility to apoptosis during brain development and after traumatic brain injury. J Neurosci 2001, 21:7439–7446
36. Donovan M, Cotter TG: Caspase-independent photoreceptor apoptosis in vivo and differential expression of apoptotic protease activating factor-1 and caspase-3 during retinal development. Cell Death Differ 2002, 9:1220–1231
37. Wright KM, Linhoff MW, Potts PR, Deshmukh M: Decreased apoptosome activity with neuronal differentiation sets the threshold for strict IAP regulation of apoptosis. J Cell Biol 2004, 167:303–313
38. Segura MF, Sole C, Pascual M, Moubarak RS, Perez-Garcia MJ, Gozzelino R, Iglesias V, Badiola N, Bayascas JR, Llecha N, Rodriguez-Alvarez J, Soriano E, Yuste VJ, Comella JX: The long form of Fas apoptotic inhibitory molecule is expressed specifically in neurons and protects them against death receptor-triggered apoptosis. J Neurosci 2007, 27:11228–11241
39. Doonan F, Donovan M, Cotter TG: Caspase-independent photoreceptor apoptosis in mouse models of retinal degeneration. J Neurosci 2003, 23:5723–5731
40. Zeiss CJ, Neal J, Johnson EA: Caspase-3 in postnatal retinal development and degeneration. Invest Ophthalmol Vis Sci 2004, 45:964–970
41. Sanges D, Comitato A, Tammaro R, Marigo V: Apoptosis in retinal degeneration involves cross-talk between apoptosis-inducing factor (AIF) and caspase-12 and is blocked by calpain inhibitors. Proc Natl Acad Sci USA 2006, 103:17366–17371
42. Cheung EC, Melanson-Drapeau L, Cregan SP, Vanderluit JL, Ferguson KL, McIntosh WC, Park DS, Bennett SA, Slack RS: Apoptosis-inducing factor is a key factor in neuronal cell death propagated by BAX-dependent and BAX-independent mechanisms. J Neurosci 2005, 25:1324–1334
43. Muñoz-Pinedo C, Guio-Carrion A, Goldstein JC, Fitzgerald P, Newmeyer DD, Green DR: Different mitochondrial intermembrane space proteins are released during apoptosis in a manner that is coordinately initiated but can vary in duration. Proc Natl Acad Sci USA 2006, 103:11573–11578
44. Otera H, Ohsakaya S, Nagaura Z, Ishihara N, Mihara K: Export of mitochondrial AIF in response to proapoptotic stimuli depends on processing at the intermembrane space. EMBO J 2005, 24:1375–1386
45. Polster BM, Basanez G, Etxebarria A, Hardwick JM, Nicholls DG: Calpain I induces cleavage and release of apoptosis-inducing factor from isolated mitochondria. J Biol Chem 2005, 280:6447–6454
46. Yuste VJ, Moubarak RS, Delettre C, Bras M, Sancho P, Robert N, d'Alayer J, Susin SA: Cysteine protease inhibition prevents mitochondrial apoptosis-inducing factor (AIF) release. Cell Death Differ 2005, 12:1445–1448
47. Cao G, Xing J, Xiao X, Liou AK, Gao Y, Yin XM, Clark RS, Graham SH, Chen J: Critical role of calpain I in mitochondrial release of apoptosis-inducing factor in ischemic neuronal injury. J Neurosci 2007, 27:9278–9293

48. Yabe T, Kanemitsu K, Sanagi T, Schwartz JP, Yamada H: Pigment epithelium-derived factor induces pro-survival genes through cyclic AMP-responsive element binding protein and nuclear factor kappa B activation in rat cultured cerebellar granule cells: implication for its neuroprotective effect. Neuroscience 2005, 133:691–700
49. Modjtahedi N, Giordanetto F, Madeo F, Kroemer G: Apoptosis-inducing factor: vital and lethal. Trends Cell Biol 2006, 16:264–272
50. Zimmermann R, Strauss JG, Haemmerle G, Schoiswohl G, Birner-Gruenberger R, Riederer M, Lass A, Neuberger G, Eisenhaber F, Hermetter A, Zechner R: Fat mobilization in adipose tissue is promoted by adipose triglyceride lipase. Science 2004, 306:1383–1386
51. Haemmerle G, Lass A, Zimmermann R, Gorkiewicz G, Meyer C, Rozman J, Heldmaier G, Maier R, Theussl C, Eder S, Kratky D, Wagner EF, Klingenspor M, Hoefler G, Zechner R: Defective lipolysis and altered energy metabolism in mice lacking adipose triglyceride lipase. Science 2006, 312:734–737
52. Chung C, Doll JA, Gattu AK, Shugrue C, Cornwell M, Fitchev P, Crawford SE: Anti-angiogenic pigment epithelium-derived factor regulates hepatocyte triglyceride content through adipose triglyceride lipase (ATGL). J Hepatol 2008, 48:471–478
53. Farooqui AA, Horrocks LA: Brain phospholipases A2: a perspective on the history. Prostaglandins Leukot Essent Fatty Acids 2004, 71:161–169
54. Wang H, Shimoji M, Yu SW, Dawson TM, Dawson VL: Apoptosis inducing factor and PARP-mediated injury in the MPTP mouse model of Parkinson's disease. Ann NY Acad Sci 2003, 991:132–139
55. Culmsee C, Zhu C, Landshamer S, Becattini B, Wagner E, Pellecchia M, Blomgren K, Plesnila N: Apoptosis-inducing factor triggered by poly(ADP-ribose) polymerase and Bid mediates neuronal cell death after oxygen-glucose deprivation and focal cerebral ischemia. J Neurosci 2005, 25:10262–10272
56. Miramar MD, Costantini P, Ravagnan L, Saraiva LM, Haouzi D, Brothers G, Penninger JM, Peleato ML, Kroemer G, Susin SA: NADH oxidase activity of mitochondrial apoptosis-inducing factor. J Biol Chem 2001, 276:16391–16398

Role of TGF-β in proliferative vitreoretinal diseases and ROCK as a therapeutic target

Takeshi Kita[a], Yasuaki Hata[a,1], Ryoichi Arita[a], Shuhei Kawahara[a], Muneki Miura[a], Shintaro Nakao[a,b], Yasutaka Mochizuki[a], Hiroshi Enaida[a], Yoshinobu Goto[c], Hiroaki Shimokawa[d], Ali Hafezi-Moghadam[b], and Tatsuro Ishibashi[a]

[a]Department of Ophthalmology, Graduate School of Medical Sciences, Kyushu University, 3-1-1 Maidashi, Higashi-Ku, Fukuoka 812-8582, Japan; [b]Angiogenesis Laboratory, Massachusetts Eye and Ear Infirmary and Department of Ophthalmology, Harvard Medical School, 325 Cambridge Street, 3rd Floor, Boston, MA 02114; [c]Department of Occupational Therapy, Faculty of Rehabilitation, International University of Health and Welfare, 137-1 Enokizu, Okawa, Fukuoka 831-8501, Japan; and [d]Department of Cardiology, Graduate School of Medicine, Tohoku University, 1-1 Seiryo-Machi, Aoba-Ku, Sendai 980-8575 Japan

Edited by Jeremy Nathans, Johns Hopkins University School of Medicine, Baltimore, MD, and approved August 6, 2008 (received for review April 30, 2008)

Cicatricial contraction of preretinal fibrous membrane is a cause of severe vision loss in proliferative vitreoretinal diseases such as proliferative diabetic retinopathy (PDR) and proliferative vitreoretinopathy (PVR). TGF-β is overexpressed in the vitreous of patients with proliferative vitreoretinal diseases and is also detectable in the contractile membranes. Therefore, TGF-β is presumed to contribute to the cicatricial contraction of the membranes, however, the underlying mechanisms and TGF-β's importance among various other factors remain to be elucidated. Vitreous samples from PDR or PVR patients caused significantly larger contraction of hyalocyte-containing collagen gels, compared with nonproliferative controls. The contractile effect was strongly correlated with the vitreal concentration of activated TGF-β2 ($r = 0.82$, $P < 0.0001$). PDR or PVR vitreous promoted expression of α-smooth muscle actin (α-SMA) and phosphorylation of myosin light chain (MLC), a downstream mediator of Rho-kinase (ROCK), both of which were dramatically but incompletely suppressed by TGF-β blockade. In contrast, fasudil, a potent and selective ROCK inhibitor, almost completely blocked the vitreous-induced MLC phosphorylation and collagen gel contraction. Fasudil disrupted α-SMA organization, but it did not affect its vitreal expression. *In vivo*, fasudil significantly inhibited the progression of experimental PVR in rabbit eyes without affecting the viability of retinal cells by electroretinographic and histological analyses. These results elucidate the critical role of TGF-β in mediating cicatricial contraction in proliferative vitreoretinal diseases. ROCK, a key downstream mediator of TGF-β and other factors might become a unique therapeutic target in the treatment of proliferative vitreoretinal diseases.

proliferative diabetic retinopathy | proliferative vitreoretinopathy | fibrosis | wound healing

Proliferative vitreoretinal diseases, such as proliferative diabetic retinopathy (PDR) and proliferative vitreoretinopathy (PVR), remain common causes of severe vision loss despite recent advancements in vitreoretinal surgery (1, 2). A better understanding of the pathogenesis of these diseases is critical for the development of urgently needed new pharmacologic treatments.

Excessive wound healing in proliferative vitreoretinal diseases leads to formation of cicatricial preretinal fibrous membranes. This process is characterized by the migration and proliferation of various cell types, including hyalocytes, retinal pigment epithelial cells (RPE), glial cells, and myofibroblast-like cells of unknown origin. These cells organize into the proliferative membrane (3, 4). Hyalocytes are found in the cortical vitreous in the vicinity of the inner retinal surface (5). Morphological studies suggest that hyalocytes may belong to the monocyte/macrophage lineage (6, 7). Hyalocytes are thought to originate from the bone marrow and differentiate in the vitreous (8). Under physiologic conditions, hyalocytes contribute to the transparency of the vitreous (9), however, they may also be involved in diseases of the vitreoretinal interface (3, 10). Specifically, in diabetic eyes, hyalocytes are found in higher numbers and their morphology is distinct from that in normal eyes (11).

Contraction of the proliferative membranes causes retinal detachment, which leads to photoreceptor apoptosis and ultimately to vision loss. Growth factors, such as TGF-β, PDGF (12, 13), insulin-like growth factor-1 (IGF-1) (13), and endothelins (14) regulate the cicatricial contraction of the preretinal membranes.

TGF-β is a multifunctional cytokine, regulating pivotal biological responses, such as differentiation, apoptosis, migration, immune cell function, and ECM synthesis (15). TGF-β has three isoforms (TGF-β1, -β2, and -β3) and is secreted as a biologically inactive latent complex. Latent TGF-β is activated by various chemical or enzymatic treatments (16–18).

TGF-β has been implicated in tissue contraction in fibrous diseases, such as liver cirrhosis, pulmonary fibrosis, and systemic sclerosis (19). In the eye, TGF-β is overexpressed in the vitreous of patients with PDR and PVR (20, 21) and is also identified in proliferative membranes in these diseases (22). Specifically, the concentration of TGF-β2, the predominant TGF-β isoform in the posterior segment of the eye (23), significantly correlates with the severity of PVR (20). In addition, we previously showed that TGF-β2 contributes to transdifferentiation of hyalocytes into α-smooth muscle actin (α-SMA) positive myofibroblast-like cells that cause collagen gel contraction (12). Taken together, TGF-β is presumed to contribute to the contraction of the cicatricial membranes in PDR and PVR. However, the direct evidence of the effect and the importance of TGF-β among various factors in the vitreous remain to be elucidated.

Phosphorylation of myosin light chain (MLC) is associated with actin-myosin interaction to form stress fibers and contractile rings, facilitating cell contraction and motility (24, 25). Rho-kinase (ROCK), a target protein of Rho, is implicated in cell adhesion, migration, proliferation, and apoptosis. ROCK regulates MLC phosphorylation both directly and via inactivation of the MLC phosphatase (25, 26). Previously we showed that TGF-β2 activates Rho, leading to MLC phosphorylation in hyalocytes (12, 21). A potent and selective ROCK inhibitor,

Author contributions: T.K., Y.H., S.N., A.H.-M., and T.I. designed research; T.K., Y.H., R.A., S.K., M.M., Y.M., H.E., and Y.G. performed research; Y.G. and H.S. contributed new reagents/analytic tools; T.K., Y.H., S.N., A.H.-M., and T.I. analyzed data; and T.K., Y.H., S.N., and A.H.-M. wrote the paper.

The authors declare no conflict of interest.

This article is a PNAS Direct Submission.

[1]To whom correspondence should be addressed. E-mail: hatachan@med.kyushu-u.ac.jp.

This article contains supporting information online at www.pnas.org/cgi/content/full/0804054105/DCSupplemental.

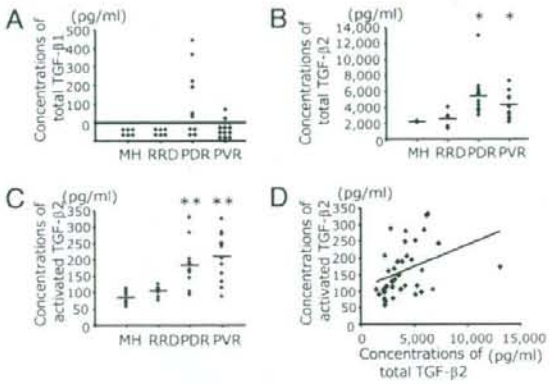

Fig. 1. Concentrations of total and activated TGF-β1 and -β2 protein in the vitreous. (*A*) Concentrations of total TGF-β1 in the vitreal samples were measured by ELISA (MH, $n = 6$; RRD, $n = 6$; PDR, $n = 12$; and PVR, $n = 11$). (*B* and *C*) Concentrations of total TGF-β2 (*B*) and activated TGF-β2 (*C*). (MH, $n = 6$; RRD, $n = 6$; PDR, $n = 12$; and PVR, $n = 12$). *: PDR vs. MH, $P = 0.0007$; PDR vs. RRD, $P = 0.003$; PVR vs. MH, $P = 0.002$; and PVR vs. RRD, $P = 0.049$. **: PDR vs. MH, $P = 0.005$; PDR vs. RRD, $P = 0.015$; PVR vs. MH, $P = 0.002$; and PVR vs. RRD, $P = 0.005$ (Mann-Whitney *U*-test). (*D*) Correlation between the concentrations of total and activated TGF-β2 ($r = 0.37$, $P = 0.026$).

fasudil, suppresses TGF-β2-induced MLC phosphorylation and collagen gel contraction by hyalocytes (12).

In the present study, we investigate the role of TGF-β in mediating cicatricial contraction in proliferative vitreoretinal diseases using vitreous samples. Furthermore, we demonstrate the underlying molecular mechanisms and the central role of ROCK in the cicatrical contraction, downstream of TGF-β and other growth factors.

Results

TGF-β1 and -β2 Concentration in the Vitreous. We quantified the concentration of total (activated and latent) TGF-β1 and -β2 protein in vitreous from PDR or PVR patients and nonproliferative controls [macular hole (MH) or rhegmatogenous retinal detachment (RRD)]. Total TGF-β1 was not detectable in MH or RRD samples. In contrast, total TGF-β1 was found in some of PDR and PVR samples (PDR, 115.4 ± 44.6 pg/ml; PVR, 12.7 ± 8.5 pg/ml) (Fig. 1*A*). Activated TGF-β1 was not detectable in any of the groups (data not shown). Vitreal concentrations of total TGF-β2 in patients with PDR (5563 ± 765 pg/ml) and PVR (4283 ± 455 pg/ml) were significantly higher than those from MH (2213 ± 34.3 pg/ml) and RRD (2643 ± 403 pg/ml) (Fig. 1*B*). Analogously, the vitreal concentrations of activated TGF-β2 in patients with PDR (180.3 ± 20.4 pg/ml) and PVR (211.9 ± 21.5 pg/ml) were significantly higher than those from MH (86.8 ± 9.1 pg/ml) and RRD (105.2 ± 7.4 pg/ml) (Fig. 1*C*). In addition, there was a significant correlation between the concentrations of total and activated TGF-β2 protein in the vitreous ($r = 0.37$, $P = 0.026$) (Fig. 1*D*). The average percent ratio of activated TGF-β2 to total TGF-β2 of all vitreal samples was 4.5 ± 0.3%.

Role of TGF-β in Vitreous-Induced Collagen Gel Contraction. Recombinant TGF-β2 caused significant contraction of hyalocyte-containing collagen gels (58.7 ± 0.4% compared to the diameter of the control gels, $n = 24$, $P < 0.0001$; paired *t*-test), which was effectively blocked (99.8 ± 0.3%, $P < 0.0001$ vs. TGF-β2) with an anti-TGF-β (-β1, -β2, and -β3) mAb, while a mouse control IgG did not affect the TGF-β2-induced contraction (Fig. 2*A*).

Vitreous samples with proliferative (PDR, 64.6 ± 2.1% and PVR, 61.8 ± 2.1%) and nonproliferative (MH, 74.1 ± 1.7% and RRD, 73.9 ± 1.5%) vitreoretinal diseases significantly decreased the diameter of hyalocyte-containing collagen gels, compared with DMEM-treated control ($n = 6$, $P < 0.0001$ in each group; Mann-Whitney *U*-test). Furthermore, PDR or PVR vitreous caused hypercontraction of hyalocyte-containing collagen gels as compared with vitreous with MH (PDR, $P = 0.01$ and PVR, $P = 0.007$; Mann-Whitney *U*-test) or RRD (PDR, $P = 0.007$ and PVR, $P = 0.004$). The vitreous-induced collagen gel contraction was significantly suppressed with an anti-TGF-β mAb (MH, 99.1 ± 0.3%; RRD, 94.2 ± 1.6%; PDR, 86.2 ± 3.4% and PVR, 86.6 ± 1.5%, $P < 0.0001$ in each; paired *t*-test) (Fig. 2 *A* and *B*), but was not affected by a mouse control IgG [supporting information (SI) Fig. S1]. The concentration of activated TGF-β2 in the vitreal samples showed a strong correlation with the reduction in diameter of the gels ($r = 0.82$, $P < 0.0001$). However, there was no significant correlation between the

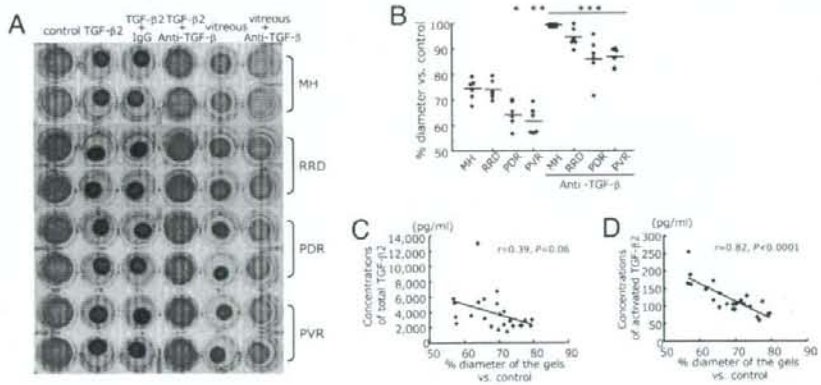

Fig. 2. Role of TGF-β in vitreous-induced collagen gel contraction. (*A*) Hyalocyte-containing collagen gels were exposed to control (DMEM), recombinant TGF-β2 (0.3 nM), or patient vitreous, with anti-TGF-β mAb (10 ng/ml) or control IgG (10 ng/ml) ($n = 6$ in each group). Two representative wells per condition, 3 days after stimulation, are shown. (*B*) The diameters of the gels treated with vitreous (lane 5 in *A* and vitreous with anti-TGF-β mAb lane 6 in *A* were measured and expressed as a percentage of the diameter of control (lane 1 in *A*). *, $P = 0.01$ vs. MH and $P = 0.007$ vs. RRD; **, $P = 0.007$ vs. MH and $P = 0.004$ vs. RRD; ***, $P < 0.0001$ vs. each disease without anti-TGF-β mAb. (*C* and *D*) The correlation of the diameters of the gels with concentration of total TGF-β2 in the vitreous ($n = 24$, $r = 0.39$, $P = 0.06$) (*C*) and with activated TGF-β2 ($n = 24$, $r = 0.82$, $P < 0.0001$) (*D*).

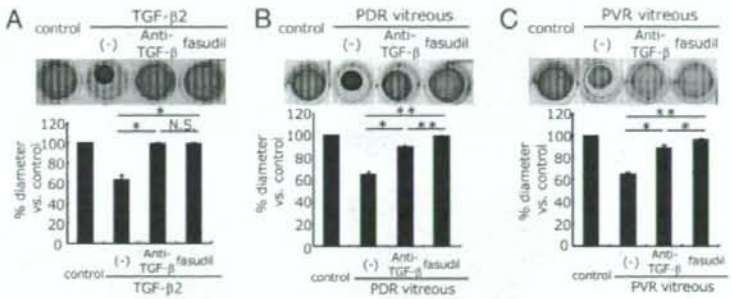

Fig. 3. Suppressive effect of fasudil on PDR/PVR-induced collagen gel contraction. Hyalocyte-containing collagen gels were stimulated with recombinant TGF-β2 (*A*), PDR vitreous (*B*), or PVR vitreous (*C*) ($n = 3$, each group) with or without anti-TGF-β mAb or fasudil (20 μM) for 3 days. Thereafter, the gels were photographed and the diameter of the gels was measured and statistically analyzed. Representative results are shown. *, $P < 0.05$; **, $P < 0.01$; NS, not significant (paired *t* test).

concentration of total TGF-β2 and the gel diameter ($r = 0.39$, $P = 0.06$) (Fig. 2 *C* and *D*).

Impact of ROCK Inhibition on PDR/PVR-Induced Collagen Gel Contraction. Both TGF-β inhibition with a mAb and ROCK inhibition with fasudil almost completely suppressed the TGF-β2-induced collagen gel contraction (average diameter of the gels compared with the medium-treated controls: TGF-β2, 63.4 ± 4.1%; TGF-β2/anti-TGF-β, 99.3 ± 0.4%; TGF-β2/fasudil, 98.9 ± 0.7%) (Fig. 3*A*). However, TGF-β blockade significantly but incompletely inhibited the collagen gel contraction, induced by PDR/PVR vitreal samples (PDR, 64.4 ± 2.3%; PDR/anti-TGF-β, 89.5 ± 1.1%; PVR, 64.6 ± 0.3%; and PVR/anti-TGF-β, 88.2 ± 2.8%). In comparison, fasudil almost completely suppressed the contraction of collagen gels treated with PDR (99.3 ± 0.5%) and PVR (95.9 ± 1.5%) samples. The impact of fasudil on PDR/PVR-induced collagen gel contraction was significantly higher than that of TGF-β blockade (Fig. 3 *B* and *C*).

Role of TGF-β in the PDR/PVR-Induced α-SMA Expression. Recombinant TGF-β2 enhanced the expression of α-SMA protein, an indicator of myofibroblastic transdifferentiation (2.5 ± 0.2 folds compared to medium-treated control), which was significantly reduced by anti-TGF-β mAb treatment (1.1 ± 0.04 folds). However, fasudil did not reduce TGF-β2-induced α-SMA up-regulation (2.6 ± 0.3 folds) (Fig. 4*A*). The PDR and PVR vitreal samples caused a significant 1.9 ± 0.1 and 1.8 ± 0.1 fold increase in α-SMA expression compared with the medium-treated controls. These increases in α-SMA expression were significantly suppressed by TGF-β inhibition (PDR/anti-TGF-β, 1.1 ± 0.1 folds and PVR/anti-TGF-β, 1.1 ± 0.1 folds). However, fasudil did not significantly reduce the increase in α-SMA expression, caused by PDR (1.95 ± 0.1 folds) or PVR (1.9 ± 0.1 folds) vitreous (Fig. 4 *B* and *C*). Immunohistochemical analysis of the hyalocyte-containing collagen gels showed increased α-SMA expression with TGF-β2 and PDR vitreous treatment (Fig. S2 *A*, *B*, and *D*). Fasudil disrupted α-SMA organization without affecting its expression (Fig. S2 *C* and *E*).

Impact of ROCK Inhibition on Vitreous-Induced MLC Phosphorylation. MLC phosphorylation was significantly increased in the presence of recombinant TGF-β2 (3.3 ± 0.2 folds) (Fig. 5*A*), PDR vitreous (2.8 ± 0.3 folds) (Fig. 5*B*) and PVR vitreous (2.6 ± 0.3 folds) (Fig. 5*C*), compared with medium-treated controls. TGF-β blockade significantly suppressed MLC phosphorylation, induced by TGF-β2 (1.01 ± 0.06 folds), PDR (1.2 ± 0.06 folds), and PVR (1.1 ± 0.1 folds) vitreous. In comparison, fasudil nearly abolished MLC phosphorylation, induced by TGF-β (0.03 ± 0.01 fold), PDR (0.03 ± 0.01 fold), and PVR (0.07 ± 0.03 fold) vitreous.

Impact of ROCK Inhibition on *In Vivo* Experimental PVR. In the vehicle-treated controls, PVR progressed with time up to 14 days after induction (Fig. 6*A*). Fasudil at a final intravitreal concentration of 10 μM inhibited only the early progression of PVR up

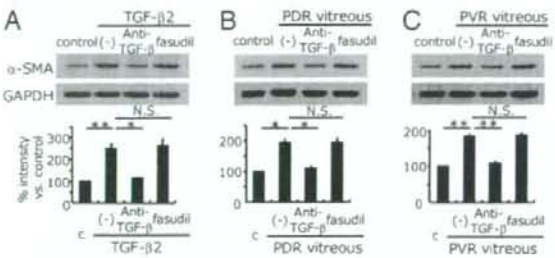

Fig. 4. Role of TGF-β in the enhanced vitreous-induced α-SMA expression. The gels from Fig. 3 were dissolved and the cells were isolated and lysed. α-SMA expressions were examined by Western blot analysis. Loaded cell lysates in *A*, *B*, and *C* were from the gels in Fig. 3 *A*, *B*, and *C*, respectively. Representative blots are shown. Signal intensities were quantified and expressed as percentages of the α-SMA/GAPDH ratio compared with control (treated with DMEM). *, $P < 0.05$; **, $P < 0.01$; NS, not significant (paired *t* test).

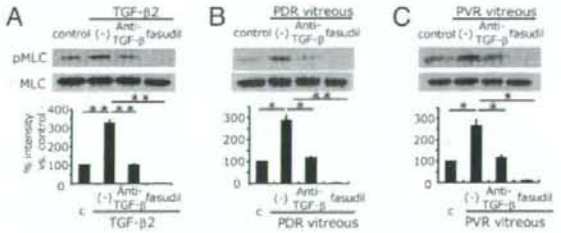

Fig. 5. Impact of fasudil on vitreous-induced MLC phosphorylation. After pretreatment with or without anti-TGF-β mAb or fasudil, hyalocytes were stimulated with recombinant TGF-β2 (*A*), vitreous with PDR (*B*), or vitreous with PVR (*C*) for 24 h ($n = 3$, each). Western blot analysis was performed to detect phosphorylated MLC (pMLC). Lane-loading differences were normalized by MLC. Signal intensities were quantified and expressed as percentages of the pMLC/MLC ratio compared with control (treated with DMEM). *, $P < 0.05$; **, $P < 0.01$.

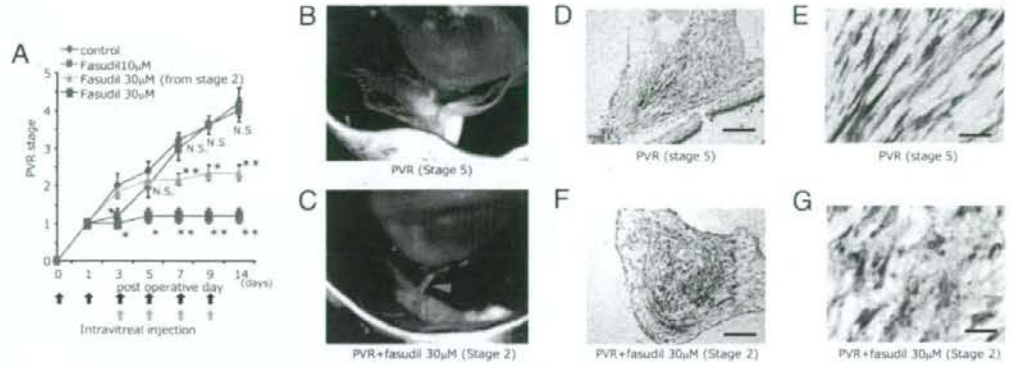

Fig. 6. Experimental PVR in rabbit eyes. (*A*) Therapeutic potential of fasudil in reducing the progression of experimental PVR. PVR was classified into six stages (0–5). Rhombus, vehicle ($n = 5$); purple square, fasudil 10 μM ($n = 5$); trigone, fasudil 30 μM from stage 2 ($n = 6$); blue square, fasudil 30 μM ($n = 5$). *, $P < 0.05$; **, $P < 0.01$; , not significant vs. vehicle. (*B* and *C*) Tractional retinal detachment because of formation and cicatricial contraction of preretinal proliferative membrane was observed by stereomicroscopy in vehicle-treated eyes (stage 5 PVR). (*D* and *F*) In contrast, intravitreal membranes adhered to the retina without causing retinal detachment (arrowhead) in 30 μM fasudil-treated eyes with stage 2 PVR. Micrographs depict α-SMA expression (brown) in preretinal proliferative membrane with stage 5 PVR (*D*) and stage 2 PVR (*F*) by immunohistochemical analysis. (Scale bar, 200 μm.) (*E* and *G*) Magnified images of *D* and *F*, respectively. (Scale bar, 10 μm.)

to the third day after disease induction. In contrast, fasudil at a concentration of 30 μM effectively suppressed the progression of the PVR from day 3 up to day 14. In addition, treatment of stage-2 PVR with fasudil, from the third or fifth day after induction, when proliferative membranes have already formed and adhered to retinal tissue, effectively blocked PVR progression. The concentrations of both total TGF-β1 and -β2 and activated TGF-β2 were significantly elevated in the vitreous with stage-5 PVR compared with control vitreous collected before disease induction (Fig. S3 *A–C*). Activated TGF-β1 was not detectable in any sample (data not shown). In the vehicle-treated eyes, contractile proliferative membranes formed (stage-5 PVR), causing total retinal detachment (Fig. 6*B*). In contrast, in the eyes treated with 30 μM fasudil from stage-2 PVR, stereomicroscopy revealed noncontractile membranes that were adherent to the retinal surface (Fig. 6*C*). Immunohistochemistry revealed expression and organization of α-SMA in the contractile preretinal proliferative membranes in the vehicle-treated eyes (Fig. 6 *D* and *F*). In fasudil-treated eyes, α-SMA was similarly expressed, however, its organization was disrupted and the membranes were noncontractile (Fig. 6 *E* and *G*).

Lack of Apparent Toxicity of Fasudil in Retinal Structure and Function. Animals were treated with repeated intravitreal injections of fasudil at 10- or 30-μM concentrations and 28 days later electroretinography and histology were performed. Electroretinographic analysis did not show a significant difference between the mean amplitude and latency of 2-Hz b-wave among the vehicle-treated animals (204.8 $\pm$ 4.6 mV and 28.1 $\pm$ 0.4 msec) and 10 μM (203.6 $\pm$ 7.2 mV and 28.0 $\pm$ 0.2 msec) and 30 μM among the fasudil-treated animals (200.9 $\pm$ 3.9 mV and 28.2 $\pm$ 0.4 msec) (Fig. S4*A*). The morphological examination of the eyes that were injected with 30 μM fasudil did not show signs of retinal damage or inflammatory cell infiltration in light microscopy or transmission EM (Fig. S4 *B–E*). Furthermore, TUNEL positive cells were found in the outer and inner nuclear layers of detached retinas from eyes with PVR, while no TUNEL positivity was found in 30 μM fasudil-treated eyes (Fig. S4 *F* and *G*). Unlike in humans and rodents, in rabbits blood vessels are limited to the medullary ray. Therefore, electroretinographic and histological analysis were also performed in fasudil-treated rats. Intravitreal fasudil did not show any obvious toxicity up to 100 μM concentration (Fig. S5). Furthermore, while 30 μM fasudil slightly but significantly reduced serum-induced proliferation of cultured rabbit conjunctival fibroblasts, the same concentration of fasudil did not affect the number of cells with serum-free DMEM or control vitreous (Fig. S6).

Discussion

This study elucidates the contractile property of human vitreous and provides direct evidence for the critical role of TGF-β in the pathogenesis of proliferative vitreoretinal diseases such as PDR and PVR. Furthermore, we demonstrate the therapeutic potential of fasudil, a potent and selective ROCK inhibitor, in the management of these diseases.

Vitreous from patients with PDR/PVR significantly enhanced contraction of hyalocyte-containing collagen gels, compared with vitreous from patients with nonproliferative diseases. This suggested the existence of vitreal factors that initiate a cascade of events leading to cicatricial contraction of the proliferative membranes in PDR/PVR patients. This insight is of clinical relevance, as it indicates that removal of the vitreous, i.e., through vitrectomy, would diminish the pathogenic factors and might be an effective treatment in a subset of patients with these diseases.

PDR/PVR-induced collagen gel contraction was dramatically suppressed by TGF-β blockade, emphasizing the central role of this cytokine in the events that lead to cicatricial contraction of the proliferative membranes. Our results further indicate that TGF-β2 is the predominantly responsible isoform in the pathogenesis. This may be because of the fact that the concentrations of total and activated TGF-β1 were negligibly low, compared with those of TGF-β2, in line with previous reports (20, 23). Furthermore, there was a strong correlation between the concentrations of activated TGF-β2 and the contractile effects, emphasizing the important role of this isoform in the pathology of PDR or PVR.

Vitreous from patients with nonproliferative diseases such as MH and RRD also caused significant collagen gel contraction, albeit substantially less than vitreous from PDR or PVR patients, which was effectively suppressed by TGF-β blockade. TGF-β is constitutively expressed in the vitreous at much lower concentrations than found in PDR/PVR patients. TGF-β contributes to the ocular immune privilege (27), and its expression under normal conditions suggests that normal vitreous might also have contractile properties. However, even though normal vitreous

and vitreous in nonproliferative diseases have contractile potential, without proliferative membranes, retinal traction may not occur *in vivo*. This suggests that the formation of proliferative membranes, which is regulated by cytokines other than TGF-β, including PDGF (6), hepatocyte growth factor (HGF) (28), and monocyte chemotactic protein-1 (MCP-1) (29), is also critical in the pathogenesis of proliferative vitreoretinal diseases.

Collagen gel contraction strongly correlated with the concentration of activated TGF-β2 in the vitreous, but not with that of total (activated + latent) TGF-β2. Our results suggest that only activated TGF-β2 in the vitreous causes collagen gel contraction, while latent TGF-β2 may serve as a precursor pool for the generation of activated TGF-β2. In addition, there was a mild but significant correlation between activated and total TGF-β2. Therefore, the significantly elevated concentration of total TGF-β2 in the vitreous in proliferative vitreoretinal diseases may also be clinically relevant.

Our results provide novel molecular insight into the mechanism of contraction in PDR/PVR. PDR/PVR vitreous enhanced α-SMA expression and MLC phosphorylation, both of which were dramatically suppressed by TGF-β blockade. This suggests that PDR/PVR vitreous may exert their procontractile property by furthering myofibroblastic transdifferentiation or MLC phosphorylation in targeted cells, such as hyalocytes. Furthermore, our results single out TGF-β as one of the main factors responsible for the procontractile property of PDR/PVR vitreous. However, other factors may also significantly contribute to the cicatricial contraction, as TGF-β blockade does not abolish the procontractile property of PDR/PVR vitreous. PDGF, IGF-1, and endothelins are also thought to be involved in the cicatricial contraction of the proliferative membrane (12–14), albeit to a lesser extent than TGF-β, as suggested in the present study.

Fasudil abolished the PDR/PVR-induced collagen gel contraction. While PDR/PVR-induced α-SMA expression was unaffected by fasudil, α-SMA organization was effectively disrupted. This suggests that fasudil might diminish the contractile property of proliferative membranes by affecting α-SMA organization, in line with previous findings (30). In addition, fasudil almost completely suppressed MLC phosphorylation, a contraction-associated molecule and a mediator of TGF-β signaling. Previously we showed that PDGF causes transient MLC phosphorylation in hyalocytes and that fasudil completely blocks it (12). Furthermore, IGF-1 and endothelin-1-induced contraction are in part dependent on MLC phosphorylation through the activation of the Rho/ROCK pathway and are effectively suppressed by ROCK inhibitors (31–33). Furthermore, ROCK inhibitors reduce cell adhesion, migration, and proliferation, and ECM production, which contribute to the formation of proliferative membranes (21, 25, 26). Our results indicate that ROCK inhibition by fasudil suppresses PVR progression even after the proliferative membranes are formed and have adhered to the retina.

Because ROCK is the common downstream mediator of various growth factors, including TGF-β, which lead to cicatrical contraction, and ROCK inhibition with fasudil reduces PDR/PVR-induced contraction more strongly than TGF-β inhibition, ROCK might be a more attractive therapeutic target than TGF-β in the treatment of cicatricial contraction of preretinal membranes. Furthermore, because TGF-β is a multifunctional cytokine, its inhibition may cause considerable side effects (34). In contrast, fasudil has already proven to be relatively safe and effective in the treatment of cardiovascular diseases, including cerebral and coronary vasospasm, angina, hypertension, pulmonary hypertension, and heart failure (35).

In summary, this work demonstrates the therapeutic potential of fasudil in halting the progression of experimental PVR, without morphological or functional indication of retinal toxicity. Our results suggest that ROCK inhibition might become a therapeutic strategy in the management of proliferative vitreoretinal diseases such as PDR and PVR.

Materials and Methods

Preparation of Vitreal Samples and ELISA. This study was carried out with approval from the Institutional Review Board and performed in accordance with the ethical standards of the 1989 Declaration of Helsinki. A written informed consent was obtained from each participant. Vitreal samples (1000–1200 μl) were collected from patients who underwent vitrectomy because of MH, RRD, PDR, or PVR. Samples with obvious bleeding were excluded. Vitreal samples were immediately centrifuged and the supernatants were snap frozen. Concentrations of TGF-β1 or -β2 in the vitreous were measured using human TGF-β1 or -β2 immunoassay kits (R&D Systems). The samples were treated with hydrochloric acid before measuring the total (activated + latent) TGF-β. Concentrations of TGF-β isoforms <31.2 pg/ml were considered undetectable.

Cell Culture. Hyalocytes were isolated and cultured from bovine eyes (21). Cultured hyalocytes obtained between four and seven passages with normal morphology were used in experiments.

Collagen Gel Contraction Assay. A mixture (0.5 ml) of hyalocytes, type I collagen (Koken Co. Ltd., Tokyo Japan), two different reconstitution buffers, and distilled water (final cell density, 2×10^5 cells/ml) was added to a 24-multiwell plate (36). After 48 h incubation with DMEM containing 10% FBS, the cells were starved with DMEM without any serum overnight. Following the 30-min pretreatment of both the cells and vitreal samples with or without anti-TGF-β (-β1, -β2, and -β3) mAb (10 ng/ml, R&D Systems) or fasudil (20 μM, generous gift of Asahi Kasei Pharma Corp., Tokyo, Japan), the cells were stimulated with recombinant TGF-β2 (0.3 nM, Sigma-Aldrich, Tokyo, Japan) or undiluted vitreal samples (300 μl/well). Mouse IgG (10 ng/ml, Sigma-Aldrich) was added for confirming the absence of nonspecific suppression of the contraction by anti-TGF-β mAb. The collagen gel diameter was measured 3 days after stimulation. The gels were dissolved by collagenase and the cells were isolated and lysed. The protein extracts were subjected to Western blot analysis for the detection of α-SMA (1:2000, Sigma-Aldrich) (36). Lane-loading differences were normalized by GAPDH (1:1000, Santa Cruz Biotechnology, Santa Cruz, CA). Signal intensities were quantified using ImageJ.

MLC Phosphorylation. Hyalocytes were seeded in collagen-coated 12-well plates. After overnight starvation with serum free DMEM, the cells were treated with PDR or PVR vitreal samples (300 μl/well), with or without anti-TGF-β mAb or fasudil for 24 h. Total cell lysates were extracted and Western blotting was performed to detect phosphorylated MLC (Thr-18/Ser-19, Santa Cruz Biotechnology). Lane-loading differences were normalized by MLC (Santa Cruz Biotechnology).

Rabbit PVR Model. Approval for experimentation with animals was obtained from the Committee on the Ethics of Animal Experiments, Kyushu University Graduate School of Medical Science, Japan. The procedures adhered to the guidelines from the Association for Research in Vision and Ophthalmology (ARVO) for animal use in research. Experimental PVR was induced by the intravitreal injection of conjunctival fibroblasts (5×10^4 in 0.1 ml DMEM) (37). On days 0, 1, 3, 5, 7, and 9 after fibroblast injection, vehicle or fasudil, which was dissolved with 0.1 ml intraocular irrigating solution (Opeguard-MA, Senju Pharmaceutical, Osaka, Japan) at final intravitreal concentration of 0 (vehicle), 10, or 30 μM, were injected into the vitreous cavity. The eyes were examined by ophthalmoscopy on days 1, 3, 5, 7, 9, and 14 by masked observers. PVR was classified into six stages using the clinical criteria (38) (Table S1 and Fig. S7 *A–C*). An additional group of animals was treated with fasudil from stage-2 PVR, on day 3 or 5. In that group, fasudil at 30 μM concentration was injected on days 3, 5, 7, and 9. After the last examination, the rabbits were euthanized by i.v. injection of pentobarbital sodium and the eyes were enucleated.

Immunohistochemistry. Paraffin-embedded sections were incubated with mouse anti-α-SMA mAb (1:100). The rinsed sections were then subjected to peroxidase-labeled secondary Ab (1:250). Peroxidase activity was visualized using diaminobenzidine, and nuclei were counterstained with hematoxylin, observed with light microscopy.

Statistics. All results were expressed as mean ± SEM. The statistical significance of differences between groups was analyzed by Mann-Whitney *U*-test or 2-tailed Student's *t*-test. Differences were considered significant at $P < 0.05$.

SI. Further information is available in *SI Materials and Methods*.

ACKNOWLEDGMENTS. We thank Marion W. Knight and Edward F. Knight and Research to Prevent Blindness. We acknowledge Asahi Kasei Pharma Corporation, Tokyo, Japan for its generous provision of fasudil. This study was supported in part by grants from the Ministry of Education, Science, Sports and Culture, Japan (Grant-in-Aid for Scientific Research nos. 19592026, 18791283, and 18591925). This work was supported by National Institutes of Health Grants AI-050775, EY-14104, and HL-086933, a Research Fellowship Award from Bausch & Lomb, and a Fellowship Award from the Japan Eye Bank Association (to S.N.).

1. Fong DS, *et al.* (2003) American Diabetes Association: Diabetic retinopathy. *Diabetes Care* 26:599–5102.
2. Pastor JC, de la Rua ER, Martin F (2002) Proliferative vitreoretinopathy: Risk factors and pathology. *Prog Retin Eye Res* 21:127–144.
3. Kampik A, Kenyon KR, Michels RG, Green WR, de la Cruz ZC (1981) Epiretinal and vitreous membranes: Comparative study of 56 cases. *Arch Ophthalmol* 99:1445–1454.
4. Jerdan JA, *et al.* (1989) Proliferative vitreoretinopathy membranes: An immunohistochemical study. *Ophthalmology* 96:801–810.
5. Salu P, Claeskens W, De Wilde A, Hijmans W, Wisse E (1985) Light and electron microscopic studies of the rat hyalocyte after perfusion fixation. *Ophthalmic Res* 17:125–130.
6. Noda Y, *et al.* (2004) Functional properties of hyalocytes under PDGF-rich conditions. *Invest Ophthalmol Vis Sci* 45:2107–2114.
7. Lazarus HS, Hageman GS (1994) In situ characterization of the human hyalocytes. *Arch Ophthalmol* 112:1356–1362.
8. Qiao H, *et al.* (2005) The characterization of hyalocytes: The origin, phenotype, and turnover. *Br J Ophthalmol* 89:513–517.
9. Lang RA, Bishop JM (1993) Macrophages are required for cell death and tissue remodeling in the developing mouse eye. *Cell* 74:453–462.
10. Kampik A, Green WR, Michels RG, Nase PK (1980) Ultrastructual features of progressive idiopathic epiretinal membrane removed by vitreous surgery. *Am J Ophthalmol* 90:797–809.
11. Faulborn J, Dunker S, Bowald S (1998) Diabetic vitreopathy: Findings using the celloidin embedding technique. *Ophthalmologica* 212:369–376.
12. Hirayama K, *et al.* (2004) The involvement of the Rho-kinase pathway and its regulation in cytokine-induced collagen gel contraction by hyalocytes. *Invest Ophthalmol Vis Sci* 45:3896–3903.
13. Hardwick C, *et al.* (1997) Tractional force generation by porcine Müller cells stimulation by growth factors in human vitreous. *Invest Ophthalmol Vis Sci* 38:2053–2063.
14. Guidry C, Hook M (1991) Endothelins produced by endothelial cells promote collagen gel contraction by fibroblasts. *J Cell Biol* 115:873–880.
15. Massague J (1998) TGF-beta signal transduction. *Annu Rev Biochem* 67:753–791.
16. Brown PD, Wakefield LM, Levinson AD, Sporn MB (1990) Physicochemical activation of recombinant latent transforming growth factor-beta's 1, 2 and 3. *Growth Factors* 3:35–43.
17. Lyons RM, Gentry LE, Purchio AF, Moses HL (1990) Mechanism of activation of latent recombinant transforming growth factor-b1 by plasmin. *J Cell Biol* 110:1361–1367.
18. Miyazono K, Heldin CH (1989) Role for carbohydrate structures in TGF-b1 latency. *Nature* 338:158–160.
19. Border WA, Noble NA (1994) Transforming growth factor b in tissue fibrosis. *N Engl J Med* 331:1286–1292.
20. Connor TB Jr., *et al.* (1989) Correlation of fibrosis and transforming growth factor-b type 2 levels in the eye. *J Clin Invest* 83:1661–1666.
21. Kita T, *et al.* (2007) Transforming growth factor-b2 and connective tissue growth factor in proliferative vitreoretinal diseases: Possible involvement of hyalocytes and therapeutic potential of Rho kinase inhibitor. *Diabetes* 56:231–238.
22. Bochaton-Piallat ML, *et al.* (2000) TGF-beta1, TGF-beta receptor II and ED-A fibronectin expression in myofibroblast of vitreoretinopathy. *Invest Ophthalmol Vis Sci* 41:2336–2342.
23. Pfeffer BA, Flanders KC, Guerin CJ, Danielpour D, Anderson DH (1994) Transforming growth factor beta2 is the predominant isoform in the neural retina, retinal pigment epithelium-choroid and vitreous of the monkey eye. *Exp Eye Res* 59:323–333.
24. Kamm KE, Stull JT (1985) The function of myosin and myosin light chain kinase phosphorylation in smooth muscle. *Annu Rev Pharmacol Toxicol* 25:593–620.
25. Fukata Y, Amano M, Kaibuchi K (2001) Rho-Rho-kinase pathway in smooth muscle contraction and cytoskeletal reorganization of non-muscle cells. *Trends Pharmacol Sci* 22:32–39.
26. Seasholtz TM, Majumdar M, Kaplan DD, Brown JH (1999) Rho and rho kinase mediate thrombin-stimulated vascular smooth muscle cell DNA synthesis and migration. *Circ Res* 84:1186–1193.
27. Streilein JW, Wilbanks GA, Cousins SW (1992) Immunoregulatory mechanisms of the eye. *J Neuroimmunol* 39:185–200.
28. Grierson I, *et al.* (2000) Hepatocyte growth factor/scatter factor in the eye. *Prog Retin Eye Res* 19:779–802.
29. Han QH, *et al.* (2001) Migration of retinal pigment epithelial cells in vitro modulated by monocyte chemotactic protein-1: Enhancement and inhibition. *Graefes Arch Clin Exp Ophthalmol* 239:531–538.
30. Bogatkevich GS, *et al.* (2003) Contractile activity and smooth muscle a-actin organization in thrombin-induced human lung myofibroblasts. *Am J Physiol Lung Mol Physiol* 285:L334–L343.
31. Zhang X, *et al.* (2005) Multiple signaling pathways are activated during insulin-like growth factor-I (IGF-I) stimulated breast cancer cell migration. *Breast Cancer Res Treat* 93:159–168.
32. Miao L, Dai Y, Zhang J (2002) Mechanism of RhoA/Rho kinase activation in endothelin-1-induced contraction in rabbit basilar artery. *Am J Physiol Heart Circ Physiol* 283:H983–989.
33. Kernochan LE, *et al.* (2002) Endothelin-1 stimulates human colonic myofibroblast contraction and migration. *Gut* 50:65–70.
34. Blobe GC, Schiemann WP, Lodish HF (2000) Role of transforming growth factor beta in human disease. *N Engl J Med* 342:1350–1358.
35. Shimokawa H, Rashid M (2007) Development of Rho-kinase inhibitors for cardiovascular medicine. *Trends Pharmacol Sci* 28:296–302.
36. Kita T, *et al.* (2007) Functional characteristics of connective tissue growth factor on vitreoretinal cells. *Diabetes* 56:1421–1428.
37. Sakamoto T, *et al.* (1995) Inhibition of experimental proliferative vitreoretinopathy by retroviral vector-mediated transfer of suicide gene: Can proliferative vitreoretinopathy be a target of gene therapy? *Ophthalmology* 102:1417–1424.
38. Fastenberg DM, Diddie KR, Dorey K, Ryan SJ (1982) The role of cellular proliferation in an experimental model of massive periretinal proliferation. *Am J Ophthalmol* 93:565–572.

平成 20 年度　厚生労働省科学研究費補助金
感覚器障害戦略研究事業　総括・分担研究報告書

発行日　平成 21 年 4 月
発行者　財団法人テクノエイド協会
〒 162-0823
東京都新宿区神楽河岸 1-1　セントラルプラザ 4F
TEL　03-3266-6880（代表）
03-3266-6881（戦略研究推進室）
FAX　03-3266-6885